Crystal Growth and Scintillation Properties of $Cs_2NaGdBr_6:Ce^{3+}$

P. Yang*, P. Doty and X. Zhou, H. Deng, M. Rodriguez, E. V. D. van Loef and K. S. Shah

***Abstract*—Single crystals of $Cs_2NaGdBr_6$ with different Ce^{+3} activator concentrations were grown by a two-zone Bridgman method. This new compound belongs to a large elpasolite halide (A_2BLnX_6) family. Many of these elpasolite compounds have shown high luminosity, good energy resolution and excellent proportionality in comparison to traditional scintillators such as CsI and NaI; therefore, they are particularly attractive for gamma-ray spectroscopy applications. This study investigated the scintillator properties of $Cs_2NaGdBr_6:Ce^{+3}$ crystals as a new material for radiation detection. Special focus has been placed on the effects of activator concentration (0 to 50 mol.%) on the photoluminescence responses. Results of structural refinement, photoluminescence, radioluminescence, lifetime and proportionality measurements for this new compound will be reported.**

***Index Terms*—Eplasolite haildes, Photoluminescence, and radioluminescence.**

I. Introduction

Cerium activated rare-earth halides represent a new family of high performance inorganic scintillators with high luminosity, good energy resolution, and excellent proportionality in comparison to traditional scintillators such as CsI or NaI. These features are particularly attractive for advanced gamma-ray spectroscopy applications. Among many of these halide compounds, two groups of materials including tri-halides (LnX3; Ln and X are the rare-earth and the halogen elements, respectively) [1], [2] and elpasolite halides (A_2BLnX_6; A, B are two different alkali elements) [3]-[5] have been actively pursued in the past decade. Some lithium based elpasolite halide compounds have also shown very promising results for gamma and thermal neutron detection.[6],[7] The distinctive performance exhibited by these new materials has accelerated the research and development pace from basic material exploration to advanced device applications. In fact, in less than a decade single crystals of cerium doped $LaBr_3$ and Cs_2LiYCl_6 are at the verge of commercialization and are experiencing increasingly widespread use for radiation detection.

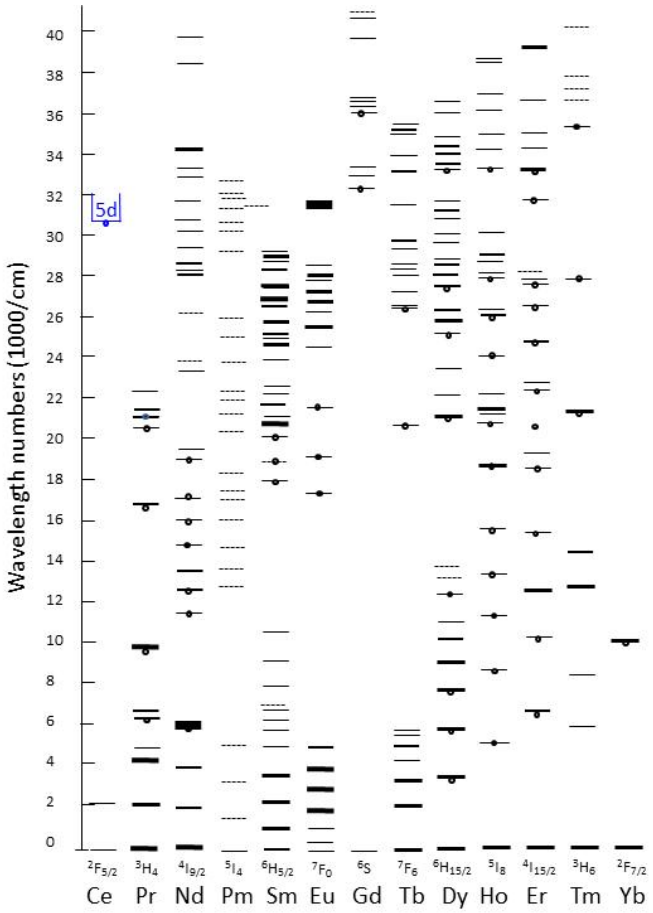

Fig. 1. Spectra and energy levels (f-f transitions) of lanthanide ions in inorganic crystals. Most of these ions, except cerium, gadolinium, and ytterbium, have many small energy gaps between sublevels and tend to produce nonradiative decay, therefore, not suitable for scintillator host. (Redrawn from G.H. Dieke, Interscience Publisher, New York, 1968).

In this study, we investigated the scintillation properties of $Cs_2NaGdBr_6$ single crystals with and without cerium activator. This new compound belongs to a large elpasolite halide family. It is expected that gadolinium compounds should have less nonradiactive interactions during the de-excitation process and are more suitable as host materials for Ce^{+3} activators because the trivalent gadolinium ion (Gd^{3+}) is one

Manuscript received June 15, 2012. This work is supported by the NNSA/DOE Office of Nonproliferation Research and Development, Proliferation Detection Program and Advanced Material Portfolio. Sandia National Laboratories is a multi-program laboratory managed and operated by Sandia Corporation, a wholly owned subsidiary of Lockheed Martin Corporation, for the U.S. Department of Energy's National Nuclear Security Administration under contract DE-AC04-94AL85000.

P. Yang* and H. Deng, M. A. Rodriguez are with Sandia National Laboratories, Albuquerque, NM 87185-0958 USA (phone: 505-821-2942; fax: 505-844-3386; e-mail: pyang@sandia.gov).

P. F. Doty, and X. Zhou are with Sandia National Laboratories, Livermore, CA 94550 USA. (e-mail: fpdoty@sandia.gov).

Edgar van Loaf and Kanai Shah are with the Radiation Monitoring Devices Inc., Watertown, MA 02472 USA, (e-mail: kshah@rmdinc.com).

of the few lanthanide ions that have few 4f energy levels with larger energy gaps between sublevels (Fig. 1). In addition, hosts have many f-f transitions may cause strong optical absorption and nonradiactive decay, as indicated by the color of these compounds. The smaller ionic size and higher atomic number (Z) of Gd^{3+}, in comparison to La^{3+} and Ce^{3+}, will also increase its density, and stopping power of this new compound. These attractive features motivated our investigation into this new gadolinium containing elpasolite halide compound. The results of structural refinement, photoluminescence, radioluminenscence, and decay time for the cerium activated $Cs_2NaGdBr_6$ (0 to 50 mol.%) will be reported.

II. EXPERIMENTAL PROCEDURE

Single crystals of $Cs_2NaGdBr_6$ were grown by the Bridgman method, using stoichiometric amounts of CsBr, NaBr, and $GdBr_3$. Nominal 2.5 mol. %, 5 mol. %, 7.5 mol. %, and 50 mol.% of $CeBr_3$ were added to substitute Gd^{3+} in the compound lattice as activator. These starting anhydrous compounds (> 99.99%) were obtained from Sigma-Aldrich, which were mixed and loaded into fused quartz ampoules in an argon-filled glove box (humidity < 0.1 ppm). These ampoules were later vacuum sealed before crystal growth. Similar to other halides, this new compound is hygroscopic and all the measurements have to be performed either in dry environment or on encapsulated samples.

The structural refinements for undoped and Ce^{3+} doped $Cs_2NaGdBr_6$ were determined by x-ray powder diffraction by a beryllium-domed technique to avoid the exposure of the material to ambient air. Data were collected using a Siemens D500 diffractometer equipped with a sealed tube x-ray source (Cu Ka) and a diffracted beam graphite monochromator. Fixed slits were employed for the measurement and generator settings were 40kV and 30mA. Typical scan parameters were 10-90^o 2θ with a step size of 0.04^o and a various count times ranging from 1 to 20 seconds. Structure refinement of isolated phases was performed using GSAS software.

The photo-excitation and emission spectra of $Cs_2NaGdBr_6$ samples were measured by a standard fluorometer (PTI QuantaMaster, Birmingham, NJ), using a Xe arc lamp as light source which coupled with a double monochromators on the excitation side and a single monochromator on the emission side. The optical quantum yield of these $Cs_2NaGdBr_6$ samples was measured, using the same excitation source with an integrating sphere [8] and a Teflon diffuser [9]. The radioluminescence spectra of $Cs_2NaGdBr_6$ were recorded using x-ray radiation from a Philips X-ray generator operated at 40 keV and 20 mA. The scintillation light was passed through a McPherson 0.2-m monochromator and detected with a cooled Burle C31034 photomultiplier tube (PMT) tube with a GaAs:Cs phtotocathode. The energy spectra and light output measurements were performed by coupling the crystals to a super bialkali R6233-100 PMT, operating at a voltage of -650 V. Pulse height spectra for the $Cs_2NaGdBr_6$ samples were recorded under 662 keV γ-ray excitation from a ^{137}Cs source. Scintillation decay time spectra were measured under 511 keV γ-ray excitation (^{22}Na source), using the time-correlated single photon counting technique. All these scintillation characterizations were measured at room temperature.

III. RESULTS AND DISCUSSION

A. Single Crystals and Structural Refinement

The cerium activated single crystals were grown in a fused quartz ampoule (1.0 cm diameter) by the Bridgman method. Cylinder shape of $Cs_2NaGd_{1-x}Ce_xBr_6$ (Figure 2) crystals were cut with a wire saw and polished with 600, 800, and 1200 grit alumina sand papers in a dry room (humidity < 0.2%) due to their hygroscopic nature.

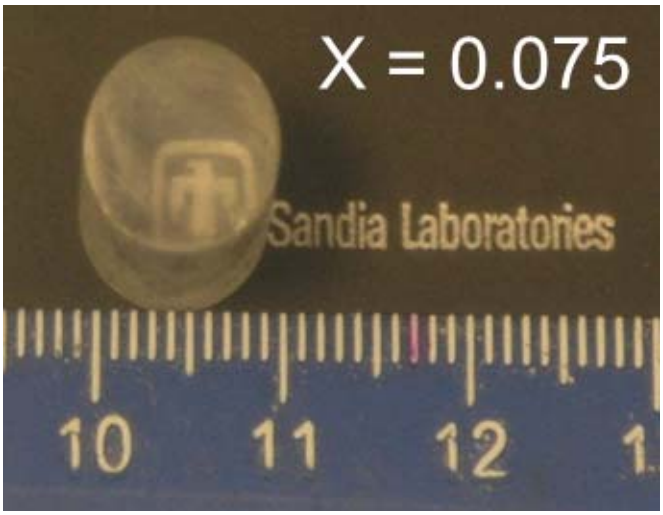

Fig. 2. 10 mm diameter $Cs_2NaGd_{0.925}Ce_{0.075}Br_6$ specimen (10 mm length) was cut and polished from a single crystal grown by the Bridgman method.

$Cs_2NaGdBr_6$ belongs to a large elpasolite halide family where many discovered compounds either possess a cubic or a hexagonal crystal structure. Powder diffraction data obtained from crushed single crystals indicated that major peaks of these samples are consistent with the Elpasolite structure. However, a trace amount of NaBr and CsBr residual phases were occasionally detected in these samples. Figure 3 shows a typical X-ray powder diffraction pattern and structural refinement results for these cerium activated $Cs_2NaGdBr_6$. Results indicated that $Cs_2NaGdBr_6$ (no Ce^{3+} doping) has a cubic structure (space group Fm3m (225)), with a lattice parameter of 11.348(1) Å and a calculated theoretical density of 4.207 g/cm^3. When the Ce^{3+} activator concentration increases from 0 to 7.5 atomic percent, the crystal symmetry does not change and the lattice parameter increases linearly from 11.348Å to 11.366Å, indicating a complete solid solution was formed within this composition range, as the larger Ce^{+3} cations substitute the smaller Gd^{+3} in the host lattice.

The potential of forming a cubic elpasolite halide has a strong advantage over the anisotropic tri-halide compounds when it comes to the crystal growth of practical sizes for detector applications. Many thermomechanical stress problems associated with the solidification process can be avoided, particularly for the growth of larger crystals. In

addition, being an optical isotropic medium can significantly reduce the amount of light scattering at grain boundaries in comparison to birefringent materials such as these tri-halide compounds. Therefore, high optical quality, low-cost polycrystalline materials can potentially be fabricated in large sizes which in turn will increase the widespread use of these high performance materials for radiation detection applications.

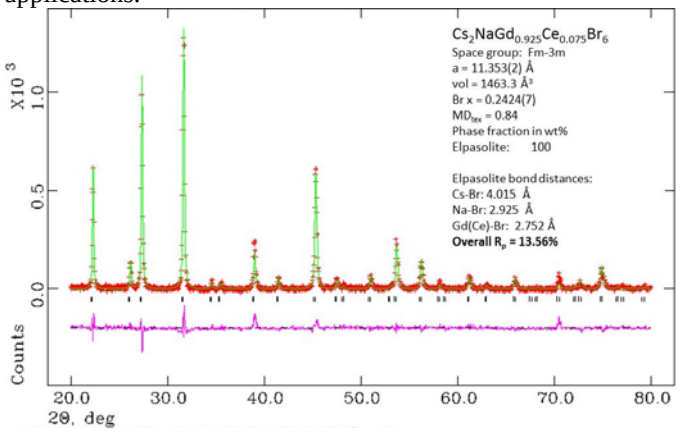

Fig. 3. X-ray diffraction pattern and structural refinement for $Cs_2NaGd_{0.925}Ce_{0.075}Br_6$. verify it is Fm-3m or Fm3m?

B. Optical Spectroscopy

Figure 4 shows optical excitation (dotted) and emission (solid) spectra collected at 346.5 nm and 427 nm for undoped $Cs_2NaGdBr_6$. Results indicate that this new compound is an intrinsic scintillator. The excitation spectrum is broad and has several peaks. Some of these peaks such as peaks at 274 nm and 313 nm resemble the gadolinium $^6I_{7/2}$-$^8S_{7/2}$ and $^6P_{7/2}$-$^8S_{7/2}$ transitions. Since Gd^{3+} occupies a centrosymmetric octahedral site (O_h) in the elpasolite halide lattice, it is anticipated that the excitation/absorption should not be very intense as purely electronic 4f-4f transitions are forbidden. The sources of the broad excitation band observed between 320 nm to 380 nm with multiple peaks are not clear. It might be attribute to lattice defects as there is no 4f-4f transition for Gd^{3+} in the range.

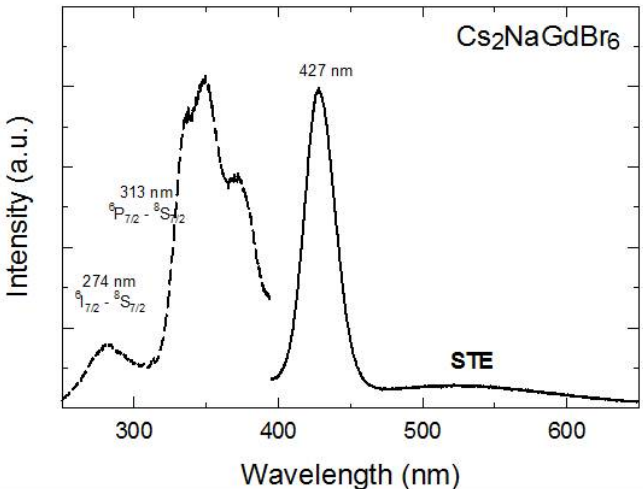

Fig. 4. The excitation and emission spectra for intrinsic $Cs_2NaGdBr_6$.

A strong emission band peaked at 427 nm is observed followed by a weak, broad band emission centered at 550 nm. The first broad peak (i.e. 427 nm) conceivably due to lattice defect emission can also be observed (not shown) when the crystal is excited by the gadolinium $^8S_{7/2}$ to $^6I_{7/2}$ transition (274 nm). This immediately suggests that lattice defects and gadolinium 4f-4f transitions play an important role in scintillation for this intrinsic scintillator. The weak and broad emission band centered at 550 nm, similar to that observed in $LaBr_3$ crystal, can be attributed to a self-trapped exciton (STE) luminescence.[5],[10]

Figure 5 shows excitation and emission spectra measured for cerium doped $Cs_2NaGd_{1-x}Ce_xBr_6$ samples. The excitation spectra shown on Fig. 5 (a) exhibit a broad excitation band from 325 nm to 380 nm, and this band widens as cerium concentration increases. The emission spectra (Fig. 5 (b)) for these samples show two broad bands peaked around 382 nm and 420 nm. This doubled peaked emission pattern can be assigned to the 5d-to-4f cerium transitions from the lowest 5d excited state to the two spin-obit split $^2F_{5/2}$ and $^2F_{7/2}$ ground state levels. The decrease in the relative intensities of the shorter wavelength emission (i.e., 382 nm) with the increase of Ce^{3+} concentration might be attributed to the self-absorption of Ce^{3+} emission. A part of the short wavelength emission is absorbed by neighboring Ce^{3+} ions and re-emitted at a longer wavelength (420 nm) leading to enhanced emission intensity.

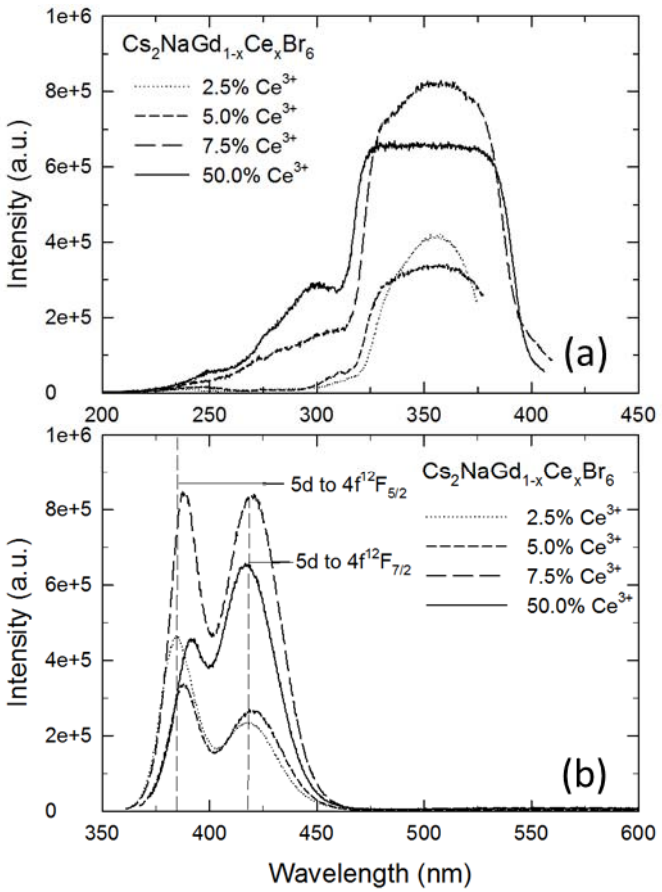

Fig. 5. Optical excitation (a) and emission (b) spectra of $Cs_2NaGd_{1-x}Ce_xBr_6$

crystals. The excitation spectra were measured at 382 nm emission for 2.5% and 5.0 % samples and 420 nm for 7.5% and 50.0% samples, while the emission spectra were collected under 351 nm excitation.

Since Ce^{3+} is an effective activator, weak STE emission detected in the intrinsic $Cs_2NaGdBr_6$ (Fig. 4.) was completely inundated by the 5d-to-4f Ce^{3+} transitions.

Optical quantum yield plays an important role in the de-excitation processes as it governs the efficiency of light output at the activator site and as such it is closely related to the luminosity of the scintillator. The quantum yield (QY) for the $Cs_2NaGd_{1-x}Ce_xBr_6$ solid solution was determined by a powder method. Prior these measurements, the accuracy of our system was confirmed by a 0.1 M quinine sulfate solution (QY = 58%). Figure 6 depicts the change of optical QY for $Cs_2NaGd_{1-x}Ce_xBr_6$ solid solution. It is evident from this figure that Ce^{3+} is an effective activator, as the QY increases from 29.3%, 48.0%, 50.2%, to 67.4% as its concentration increase from 0%, 2.5%, 5%, to 7.5%. However, when the Ce^{3+} concentration increases to 50%, the QY drops back to 60.2%, suggesting a slightly concentration quenching for the $Cs_2NaGdBr_6$ scintillator.

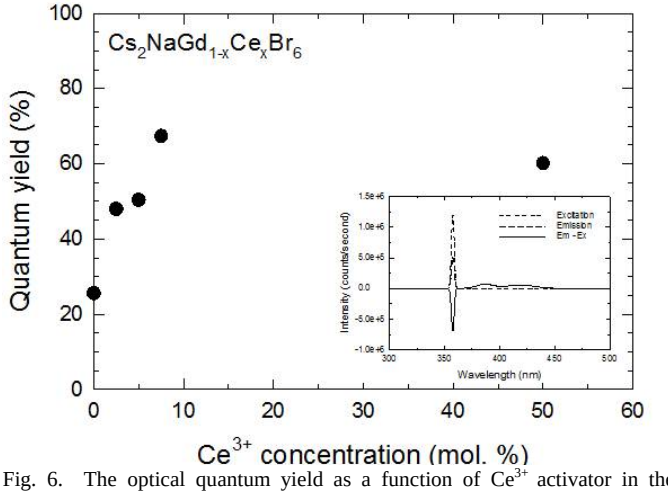

Fig. 6. The optical quantum yield as a function of Ce^{3+} activator in the $Cs_2NaGd_{1-x}Ce_xBr_6$ solid solution. Insert shows the quantum yield measurement for $Cs_2NaGd_{0.95}Ce0.05Br6$ crystal at 357 nm

C. Radioluminescence

The emission spectrum of the undoped $Cs_2NaGdBr_6$ measured under x-ray excitation exhibits a similar emission pattern as its photoluminescence spectrum (not shown), with a small and a large Gd^{3+}: $^6P_{7/2}$-$^8S_{7/2}$ emission peaks at 313 nm and 427 nm, as well as a broad STE emission band centered at 550 nm. When 5% Ce was added, the STE emission completely disappeared and the double-peak emission is due to 5d-to-4f transitions of Ce^{3+} (Fig. 7). The additional peak observed at 626 nm, same peak height of 313 nm peak, is an artifact due to a second-order grating effect from optics.

Fig. 8 shows the energy spectra and light output measurements of the $Cs_2NaGd_{0.95}Ce_{0.05}Br_6$ crystal under 662 keV gamma rays irradiation from a ^{137}Cs source. The spectrum is recorded with a shaping time of 4 μs at room temperature. Energy resolution is obtained from FWHM of the photopeak using a single Gaussian function. Results show the energy resolution of $Cs_2NaGd_{0.95}Ce_{0.05}Br_6$ at 662 keV is ~8.6%, which is still far from the energy resolution of $LaBr_3$:Ce^{3+} (2.6%)[ ] , but is comparable with that of NaI:Tl. Further improvement in the energy resolution could be achieved with high quality crystal.

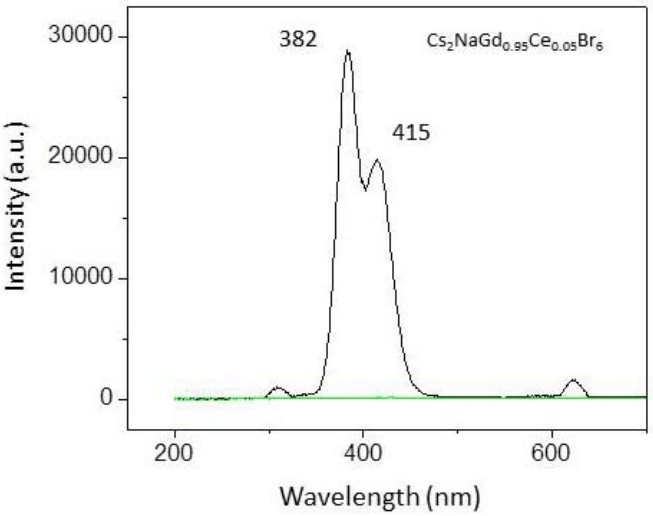

Fig. 7. Radioluminescence spectrum of $Cs_2NaGd_{0.95}Ce_{0.05}Br_6$ crystal.

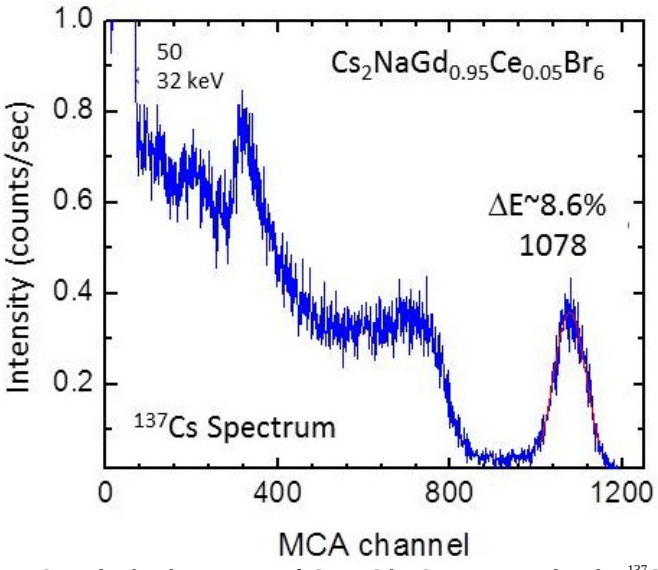

Fig. 8. Pulse height spectrum of $Cs2NaGd_{0.95}Ce_{0.05}Br_6$ crystal under ^{137}Cs excitation.

The non-proportionality of light output per energy unit versus energy of excitation measured for $Cs_2NaGdBr_6$ and $Cs_2NaGd_{0.95}Ce_{0.05}Br_6$ crystals is shown in Fig. 9. The non-proportionality is closely related to the energy resolution. Scintillators exhibits non-proportionality response will perform worse than expected energy resolution based on the photon statistics. Energy spectra of various gamma ray energies, including ^{137}Cs (32 keV, 662 keV), ^{22}Na (511, 1275 keV), ^{57}Co (122, keV) and ^{241}Am (60 keV), were used to construct the non-proportionality plot, which covers the energy range of 60-1275 keV. Each spectrum provides position of a corresponding photopeak. These values were then normalized to the incident energy and plotted relative to the ^{137}Cs 662 keV result. Results show the collected data deviate slightly from the straight line only at lower energies.

Results show that the deviations from linearity for undoped and doped (5% Ce^{3+}) samples are less than 5% and 4%, respectively. These values are comparable to cerium doped $LaBr_3$ and $LaCl_3$ which showed 4% and 7% nonproportionality in the similar energy range, but are substantially better than that of many established scintillator such as LSO (35%), NaI:Tl (20%) and CsI:Tl (20%).

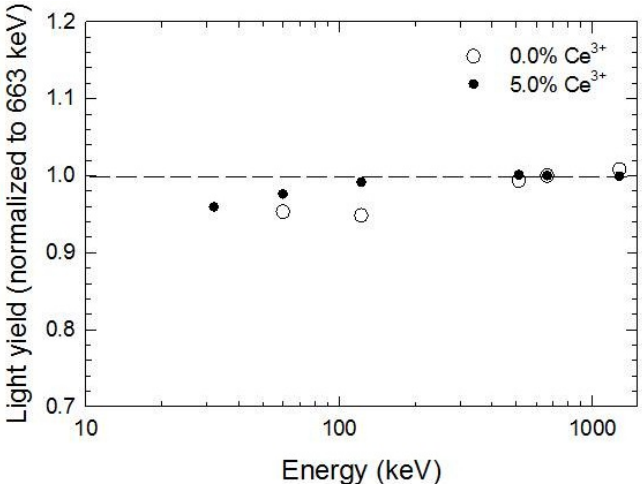

Fig. 9. The non-proportionality plots for $Cs_2NaGdBr_6$ and $Cs_2NaGd_{0.95}Ce_{0.05}Br_6$ crystals. Within the measured range the non-proportionality for $Cs_2NaGdBr_6$ (open) and $Cs_2NaGd_{0.95}Ce_{0.05}Br_6$ (close) is within 5% and 4%, respectively.

Energy resolution is particularly important for gamma-ray spectroscopy applications. Fig. 10 shows the energy resolution as a function of gamma-ray energy for undoped and 5% cerium doped $Cs_2NaGdBr_6$, collected from pulse height spectra of different radioactive isotopes. Apparently, $Cs_2NaGdBr_6$:5% Ce^{3+} has a much better energy resolution than the intrinsic $Cs_2NaGdBr_6$ scintillator. The difference in energy resolution can be attributed to the luminosity as indicated by their optical quantum yield. However, the difference becomes progressively smaller as gamma energy increases.

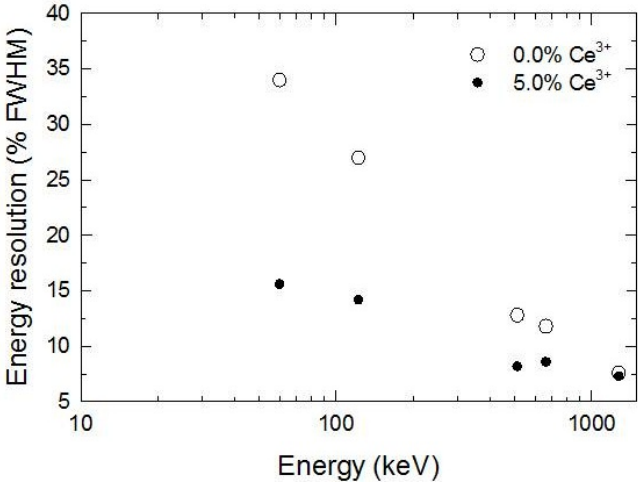

Fig. 10. Energy resolution as a function of gamma-ray energy for $Cs_2NaGdBr_6$ (open) and $Cs_2NaGd_{0.95}Ce_{0.05}Br_6$ (close) crystals.

The scintillation decay time spectrum was measured under 2.5 MeV proton beam excitation, using a single photon counting technique. The result of decay time response for the $Cs_2NaGd_{0.925}Ce_{0.075}Br_6$ crystal is given in Fig. 11. The decay curve was fitted with the sum of three exponential decay time components. These decay time components and their relative contributions to the total light output are given in Fig. 11. The relative time scale for these components reflects the energy transfer mechanisms, which will be studies in the near future.

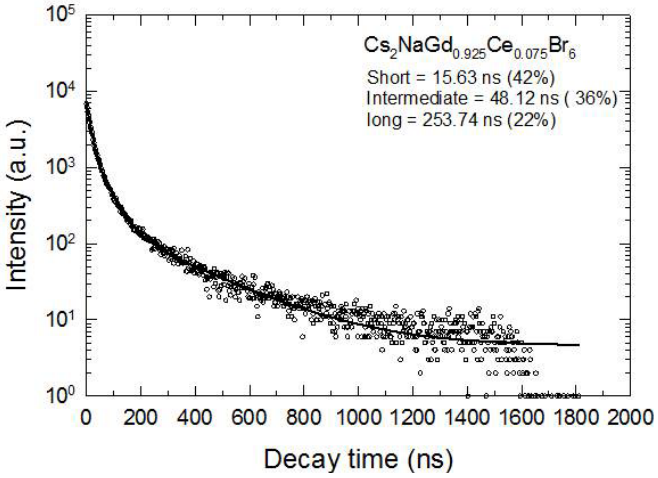

Fig. 11. Scintillation decay time spectrum for $Cs_2NaGd_{0.925}Ce_{0.075}Br_6$ crystal obtained by the proton beam excitation at 2.5 MeV. Solid line represents the fitting result.

IV. Summary

This study reported the initial investigation of $Cs_2NaGdBr_6$ scintillator as a function of cerium concentration. Results indicate that $Cs_2NaGdBr_6$ is an intrinsic scintillator. Its scintillation performance can be greatly enhanced by cerium activator. The cerium activated $Cs_2NaGdBr_6$ exhibits typical 5d-4f emissions in the 350 nm to 450 nm range, which is well matched with photomultipler tube performance. The increase of cerium concentration in the host lattice does not change the cubic elpasolite structure, but greatly enhances the optical quantum yield, linearity response and energy resolution. These results indicate that the cerium activated $Cs_2NaGdBr_6$ is well positioned to compete with traditional scintillators such as CsI and NaI in may applications. Further improvement in energy resolution is expected with improved crystal quality.

References

1. 0. Guillot-Noel, J. T. M. de Hass, P. Dorenbos, C. W. E. van Eijk, K. Kramer, and H. U. Gudel, *J. Lumin*., vol. 85, pp. 21-35, 1999.
2. K. S. Shah, J. Globo, W. H. Higgins, E. V. D. van Loef, W. W. Moses, S. E. Derenzo, and M. J. Weber, *IEEE Trans. Nucl. Sci*., vol 52(6), pp 3157-3159, 2005.
3. J. Globo, E. V. D. van Loef, W. M. Higgins, and K. S. Shah, *2006 IEEE NSS Conf. Rec*., 2006, pp 1208-1211.
4. U. Shirwadkar, J. Globo, E. V. van Loef, R. Hawrami, S. Mukhopadhyay, A. Churilov, W. M. Higgins, and K. S. Shah, *Nucl. Instr. and Meth. A*., (2010). doi:10/1016/j.nima.2010.08.050
5. G. Rooh, H. J. Kim, H. Park and S. Kim, *J. Lumin*., vol 132, pp. 713-716, 2012.
6. A. Bessiese, P. Dorenbos, C. W. E. van Eijk, K. W. Kramer and H. U. Gudel, *Nucl. Instr. and Meth. A*., vol. 537, 242-246, 2005.
7. D. W. Lee, L. C. Stonehill, A. Kimenko, J. R. Terry, S. R. Tornga, *Nucl. Instr. and Meth. A*, vol. 664, 1-5, 2012.
8. A. K. Gaigalas and L. Wang, *Res. Natl. Inst. Stand. Technol*., vol. 113, pp. 17-28, 2008.

9. L. S. Rohwer and J. E. Martin, *J. Lumin*., vol. 115, pp 77-90, 2005.
10. G. Bizarri, P. Dorenbos, *Phys. Rev. B*, vol. 75, 184302, 2007.